| Title | Spectral reuse for pilot-aided MIMO-OFDM systems over broadcast time dispersive frequency selective fading channels |
|---|---|
| Author(s) | Pan, Z; Wong, KK; Ng, TS |
| Citation | Ieee Workshop On Signal Processing Advances In Wireless Communications, Spawc, 2004, p. 348-352 |
| Issued Date | 2004 |
| URL | http://hdl.handle.net/10722/46443 |
| Rights | Creative Commons: Attribution 3.0 Hong Kong License |

# Spectral Reuse for Pilot-Aided MIMO-OFDM Systems Over Broadcast Time Dispersive Frequency Selective Fading Channels

Zhengang Pan[1],
Department of EEE
The University of Hong Kong
Pokfulam Road, Hong Kong
Email: zgpan@eee.hku.hk

Kai-Kit Wong,
Department of EEE
The University of Hong Kong
Pokfulam Road, Hong Kong
Email: kitwong@eee.hku.hk

Tung-Sang Ng,
Department of EEE
The University of Hong Kong
Pokfulam Road, Hong Kong
Email: tsng@eee.hku.hk

*Abstract* — This paper combines the techniques of multiple-input multiple-output (MIMO) antennas and orthogonal frequency division multiplexing (OFDM) to deliver high-capacity high-data-rate wireless communications over broadcast time dispersive frequency selective fading channels. For broadcast channels, multiple communications can occur at the same frequency subcarrier and time slot from one base station (BS) to many mobile stations (MS). To realize this, we develop a so-called orthogonal space division multiplexing (OSDM) scheme to decompose per-subcarrier channel into many uncoupled single-user spatial modes. In particular, the scheme is modified to improve its robustness to the channel mismatches arising from pilot-aided channel estimation and Doppler spread. Simulation results reveal that following the ESTI HiperLAN II parameters, our proposed scheme can achieve good performance with four simultaneous downlink users at Doppler spread of 40 Hz, which corresponds to mobile moving at speed of 8.5 km/h communicating at 5 GHz

.

## I. INTRODUCTION

Multiple-input multiple-output (MIMO) antennas together with orthogonal frequency division multiplexing (OFDM) has recently emerged as one of the core techniques of future-generation wireless systems that will deliver high-capacity high-data-rate reliable wireless transmission [1]–[3]. While MIMO-OFDM has been well known for improving the capacity of a single-user point-to-point communication link, it is much less understood how it could work in broadcast point-to-multipoint channels, where one base station (BS) talks to many mobile stations (MS) at the same frequency subcarrier and time slot.

In this paper, we aim to devise an orthogonal space division multiplexing (OSDM) scheme that projects multiuser signals onto orthogonal subspaces in broadcast channels so that the interference seen by all the MS is eliminated according to their spatial signatures. As a consequence, per-subcarrier of MIMO-OFDM is effectively split into a number of spatial channels. We assess the performance of the system focused on the ETSI HiperLAN II parameters, and the system performs OSDM processing based on the channel state information (CSI) estimated by pilots. Further, in order to minimize the performance degradation as a result of outdated CSI due to Doppler spread, a minimum mean square error (MMSE) receiver is used at every MS.

Promoting spectral reuse in broadcast channels traces back several decades [4] and the method is based on the so-called "dirty-paper coding" (DPC) [5]–[8]. DPC encodes the data in a way that the codes align themselves as much as possible with each other so as to maximize the sum-capacity of a broadcast channel. However, dirty-paper techniques are largely information-theoretic and worse of all, the encoding process to achieve the sum-capacity is data dependent.

Systems similar to OSDM have been considered by several authors [9]–[13]. In [9]–[11], by placing nulls at the antennas of all the unintended MS, the broadcast channel is made block diagonal so that co-channel interference (CCI) is eliminated. Later in [12, 13], MS receiver combining was also considered when placing the nulls for OSDM and it has been demonstrated that much higher diversity can be achieved. However, such good performance relies heavily on accurate CSI to be available at both the BS and MS.

This paper is organized as follows, In section II, the system model of a broadcast MIMO-OFDM is introduced. Section III presents the proposed iterative solution for per-subcarrier OSDM. Next, in Section IV, we describe the OSDM implementation in a HiperLAN II alike MIMO-OFDM system. Finally, we conclude the paper in Section V.

## II. BROADCAST MIMO-OFDM SYSTEM MODEL

The system configuration of a MIMO-OFDM broadcast system is shown in Figure 1 where signals are transmitted from one BS to $M$ MS, $n_T$ antennas are located at the BS and $n_{R_m}$ antennas are located at the $m$th MS. In the following subsections, we describe the details of signal processing at the BS and MS.

### A. Transmitter Signal Processing at BS

At time $t$, for each user, a serial-to-parallel buffer segments a sequence of information bits into $N$ parallel output streams. Each stream can be independently encoded/interleaved, and regarded as a symbol, $\{z_m[t,n] : n = 0, 1, \ldots, N-1\}$, where $z_m[t,n]$ denotes the transmitting symbol on $n$th subcarrier of user $m$ at time $t$. For simplicity, we shall omit the time index $t$ in the following discussion. Writing the symbols of all users in vector form, we have

$$z[n] = (z_1[n] \ z_2[n] \cdots z_M[n])^T, \text{ for } n = 0, \ldots, N-1 \quad (1)$$

where the superscript $T$ denotes the vector transposition. Before transmission, the multiuser data symbols, $z[n]$, are transformed by a post-multiply weight matrix, $T[n]$, so that

$$x[n] = T[n]z[n], \text{ for } n = 0, \ldots, N-1. \quad (2)$$

Afterwards, the signals, $x[n]$, are modulated by passing through $N$ parallel inverse Fourier transform (IFFT) processors. This is done by collecting the frequency domain signals

$\{x_k[0], x_k[1], \ldots, x_k[N-1]\}$ for a particular BS antenna $k$. As a result, we have the time samples $x_k(\tau)$ of an OFDM symbol at antenna $k$ on time $t$

$$x_k(\tau) = \frac{1}{\sqrt{N}} \sum_{n=0}^{N-1} x_k[n] W^{-n\tau}, \text{ for } \tau = 0, \ldots, N-1 \quad (3)$$

where $W = e^{-j2\pi/N}$. A cyclic prefix which is set to the excess delay of the radio channel is then added to each of the resulting signals to reduce the effect of intersubcarrier interference. The signal streams are finally converted from parallel-to-serial for transmission (see Figure 2).

### B. Channel Model

The transmitted signals go through a frequency selective MIMO fading channel. Here, we model the channel by using a discrete-time tap delay model [14] and assume that there are $L$ resolvable paths for each antenna pair, where $L = B\tau_{rms}$ with $B$ and $\tau_{rms}$ representing the signal bandwidth and delay spread, respectively.

Let $\mathbf{x}(\tau) = (x_1(\tau) \ x_2(\tau) \cdots x_{n_T}(\tau))^T$ and $\mathbf{y}_m(\tau) = (y_1^{(m)}(\tau) \ y_2^{(m)}(\tau) \cdots y_{n_{R_m}}^{(m)}(\tau))^T$ represent the discrete-time transmit signal vector and receive signal vector of MS $m$, respectively. Consequently,

$$\mathbf{y}_m(\tau) = \sum_{l=0}^{L-1} \mathbf{H}_m(l)\mathbf{x}(\tau - l) + \mathbf{n}_m(\tau) \quad (4)$$

where $\mathbf{n}_m(\tau)$ is the noise vector assumed to be complex additive white Gaussian noise (AWGN) with zero-mean and variance of $N_0/2$ per dimension, and $\mathbf{H}_m(l) = [h_{\ell,k}^{(m)}(l)] \in \mathbb{C}^{n_{R_m} \times n_T}$ is the $l$th tap of the MIMO channel matrix from the BS to MS $m$.

In this paper, $h_{\ell,k}^{(m)}(t, l)$ is modelled statistically as a slowly varying zero-mean complex Gaussian random process which can be generated by Jakes' model. This fading factor can be defined as $F_d T_s$, where $F_d$ and $T_s$ are Doppler spread and the duration of an OFDM symbol, respectively. Further, we assume that $h_{\ell,k}^{(m)}(l)$'s are uncorrelated for different $m, k, \ell, l$. Without loss of generality, the summation of variances of all taps of one antenna pair is set to unity.

### C. Receiver Signal Processing at MS

At the receiver side (say MS $m$), the cyclic prefix of each received signal is removed, then the time-sampled signals are passed to the fast Fourier transform (FFT) processors, as shown in Figure 3, to give the signals in frequency domain

$$y_\ell^{(m)}[n] = \frac{1}{\sqrt{N}} \sum_{\tau=0}^{N-1} y_\ell^{(m)}(\tau) W^{n\tau}, \text{ for } \tau = 0, \ldots, N-1 \quad (5)$$

where $y_\ell^{(m)}[n]$ denotes the signal received by the $\ell$th antenna of MS $m$ on the $n$th subcarrier.

Denoting $\mathbf{y}_m[n] = (y_1^{(m)}[n] \cdots y_{n_{R_m}}^{(m)}[n])^T$ as the received signal vector at MS $m$ on the $n$th subcarrier, we produce the estimate of the transmitted symbol, $z_m[n]$, by pre-multiplying $\mathbf{y}_m[n]$ to a receive antenna weight vector, $\mathbf{r}_m[n] = (r_1^{(m)}[n] \cdots r_{n_{R_m}}^{(m)}[n])^T$ to give

$$\begin{aligned} \hat{z}_m[n] &= \mathbf{r}_m^\dagger[n]\mathbf{y}_m[n] & (6) \\ &= \mathbf{r}_m^\dagger[n] (\mathbf{H}_m[n]\mathbf{x}[n] + \mathbf{n}_m[n]) & (7) \\ &= \mathbf{r}_m^\dagger[n] (\mathbf{H}_m[n]\mathbf{T}[n]\mathbf{z}[n] + \mathbf{n}_m[n]) & (8) \end{aligned}$$

where $\mathbf{H}_m[n]$ and $\mathbf{n}_m[n]$ are, respectively, the Fourier transform of $\mathbf{H}_m(l)$ and $\mathbf{n}_m(\tau)$, and the superscript $\dagger$ indicates the conjugate transposition. The IFFT and FFT together with cyclic prefix insertion convert a frequency selective fading channel into a frequency flat fading channel. As a result, signals for each subcarrier can be considered independently.

### III. SUBCARRIER OSDM

In this section, our objective is to find the antenna weights, $\mathbf{T}[n], \mathbf{r}_1[n], \ldots, \mathbf{r}_M[n]$ that can project the multiuser signals onto orthogonal subspaces and at the same time maximize the resultant channel gains of the spatial modes. Mathematically, this can be written as

$$(\mathbf{T}[n], \mathbf{r}_1[n], \ldots, \mathbf{r}_M[n])_{\text{opt}} = \arg \max_{\mathbf{T}[n], \mathbf{r}_1[n], \ldots} \sum_{m=1}^M |\lambda_m[n]|^2 \quad (9)$$

where $|\cdot|$ takes the modulus of a complex number and $\lambda_m[n]$ is defined by

$$\mathbf{r}_m^\dagger[n]\mathbf{H}_m[n]\mathbf{T}[n] = (0 \cdots 0 \ \lambda_m[n] \ 0 \cdots 0) \quad \forall m. \quad (10)$$

The optimization (9) will be performed under the assumptions that $\|\mathbf{t}_m[n]\| = \|\mathbf{r}_m[n]\| = 1 \ \forall m, n$ where we have used $\mathbf{T}[n] = (\mathbf{t}_1[n] \ \mathbf{t}_2[n] \ \cdots)$. In this case, $\lambda_m[n]$ will represent the resultant channel gain of user $m$ on the $n$th subcarrier.

### A. Iterative Pseudo-Inversion with Maximal Ratio Combining

To solve (9) and (10), we begin by first assuming that all the receive vectors are already fixed and known, and later, consider the optimization of the receive vectors. With this assumption, we define the equivalent multiuser channel matrix, $\mathbf{H}_e[n]$, as

$$\mathbf{H}_e[n] \triangleq \begin{pmatrix} \mathbf{r}_1^\dagger[n]\mathbf{H}_1[n] \\ \mathbf{r}_2^\dagger[n]\mathbf{H}_2[n] \\ \vdots \\ \mathbf{r}_M^\dagger[n]\mathbf{H}_M[n] \end{pmatrix} \in \mathbb{C}^{M \times n_T}. \quad (11)$$

Following (9) and (10), we are now required to find the optimal transmit weight matrix so that

$$\mathbf{T}[n]_{\text{opt}} = \arg \max_{\mathbf{T}[n]} \sum_{m=1}^M |\lambda_m[n]|^2 \quad (12)$$

and

$$\mathbf{H}_e[n]\mathbf{T}[n] = (0 \cdots 0 \ \lambda_m[n] \ 0 \cdots 0)^T. \quad (13)$$

Now, we define another set of weight vectors

$$\mathbf{g}_m[n] \triangleq \frac{\mathbf{t}_m[n]}{|\lambda_m[n]|} \quad \forall m \quad (14)$$

and $\mathbf{G}[n] \triangleq (\mathbf{g}_1[n] \ \mathbf{g}_2[n] \ \cdots \ \mathbf{g}_M[n])$. Then, the optimization (12) and (13) can be rewritten as

$$\mathbf{H}_e[n]\mathbf{G}[n] = \mathbf{I} \quad (15)$$

where $\mathbf{I}$ is an identity matrix. In order for (15) to exist, we must have $\text{rank}(\mathbf{H}_e[n]), \text{rank}(\mathbf{G}[n]) \geq \text{rank}(\mathbf{I}) = M$. As a result, OSDM is possible only when $n_T \geq M$. Under this condition, the optimal $\mathbf{G}[n]$ is the pseudo-inverse matrix of $\mathbf{H}_e[n]$ and can be computed as [15]

$$\mathbf{G}[n] = \mathbf{H}_e^\dagger[n] \left( \mathbf{H}_e[n]\mathbf{H}_e^\dagger[n] \right)^{-1}. \quad (16)$$

As such, the optimal antenna weights at the BS are given by

$$t_m[n] = \frac{g_m[n]}{\|g_m[n]\|} \quad \forall m. \tag{17}$$

As the CCI has been zero-forced by optimizing $\mathbf{T}[n]$, a maximal ratio combining (MRC) receiver will be the optimum receiver structure. That is,

$$\mathbf{r}_m[n] = \mathbf{H}_m[n]\mathbf{t}_m[n] \quad \forall m. \tag{18}$$

However, when the receive vectors are changed, the orthogonality will be lost. An iterative process is therefore required to tune the transmit and receive weight vectors jointly. The details of the algorithm are given as follows:

1. Initialize $\mathbf{r}_m[n] = \frac{1}{\sqrt{n_{R_m}}}[1\ 1\ \cdots\ 1]^T\ \forall m$.

2. Obtain $\mathbf{H}_e[n]$ using (11).

3. Find $\mathbf{T}[n]$ by (16) and (17).

4. For all MS $m$, update $\mathbf{r}_m[n]$ using (18).

5. Compute

$$\mathbf{r}_m^\dagger[n]\mathbf{H}_m[n]\mathbf{T}[n] = (\epsilon_1\ \cdots\ \epsilon_{m-1}\ \lambda_m[n]\ \epsilon_{m+1}\ \cdots\ \epsilon_M) \tag{19}$$

to check if $|\epsilon_i|$ is less than a preset threshold, $\epsilon_{Th}$ ($= 10^{-12}$ typically). If $|\epsilon_i| < \epsilon_{Th}\ \forall i$, the convergence is said to be achieved. Otherwise, go back to Step 2.

In this paper, we shall refer to the above iterative algorithm as iterative pseudo-inversion with MRC (PINV-MRC).

### B. Iterative Pseudo-Inversion with MMSE

PINV-MRC requires CSI to be available at both the BS and MS. In time-division-duplex (TDD) mode, this can be estimated from uplink reception using pilots (see Section IV). The estimated CSI can then be used for downlink optimization.

However, channel estimation introduces error and the estimated CSI may be outdated due to Doppler spread. To improve the robustness of the proposed OSDM method, each MS learns its own channel based on the MMSE criterion. Therefore, at the MS receiver side, instead of (18),

$$\mathbf{r}_m[n] = \mathrm{E}_t\left\{\mathbf{y}_m[t,n]\mathbf{y}_m^\dagger[t,n]\right\}^{-1}\mathrm{E}_t\left\{\mathbf{y}_m[t,n]z_m^*[t,n]\right\} \tag{20}$$

is used to remove the residual CCI caused by channel estimation error and Doppler spread. In the sequel, we shall refer to the OSDM scheme which uses (20) as PINV-MMSE to distinguish it from the original method.

### IV. PRACTICAL IMPLEMENTATION

Implementing the proposed OSDM method can be divided into three phases, which are now described as follows:

- *Uplink Pilot-Aided Channel Estimation*—For a particular antenna pair (i.e., from one antenna of a MS to a BS antenna), known pilots are placed on rectangular grid in both time and frequency subcarrier, and the separation of pilots is $M_t$ across OFDM symbols and $M_f$ across subcarriers [16]. Channel estimation is done by interpolating the channel estimates on the pilot subcarriers.

  Consider a total of $N_p$ pilots $\{a[i_k] : 0 \le k \le N_p - 1\}$ that are inserted in an OFDM block at locations $\{i_k : 0 \le k \le N_p - 1\}$. Writing $\mathbf{b} = (b[i_0]\ b[i_1]\ \cdots\ b[i_{N_p-1}])^T$ as the received signal vector at the pilot locations, we have

$$\mathbf{b} = \mathbf{AWh} + \mathbf{n} \tag{21}$$

where $\mathbf{A} = \mathrm{diag}(a[i_0], a[i_1], \ldots, a[i_{N_p-1}])$ and $\mathbf{W}$ is an $N_p \times L$ Fourier transform matrix with entries $[\mathbf{W}]_{kl} = W^{ikl}$ and $\mathbf{h} = (h(0)\ h(1)\ \ldots\ h(L-1))^T$ represents fading coefficients of the channel taps. $\mathbf{n}$ is the channel noise. With $N_p \ge L$, we can estimate $\mathbf{h}$ by a maximum likelihood (ML) channel estimator, given by

$$\hat{\mathbf{h}}_{ML} = (\mathbf{W}^\dagger\mathbf{W})^{-1}\mathbf{W}^\dagger\mathbf{A}^\dagger\mathbf{b}. \tag{22}$$

The above single-input single-output (SISO) channel estimation can be used for MIMO scenario through proper pilot placements. In this paper, we use a diagonal approach in time domain so that within a pilot-inserted OFDM symbol, only one antenna of a MS can occupy the pilot subcarriers, which essentially reduces MIMO channel estimation into multiple independent SISO channel estimation, which can be dealt by (22) as described before (for details, see also [16]).

- *Downlink BS Optimization*—The CSI estimated during the uplink frame is used to compute $\hat{\mathbf{H}}_m[n]$. Then, the algorithm (Steps 1-5 in Section III-A) is used to optimize $\mathbf{T}[n]$. Once, $\mathbf{T}[n]$'s are computed, they will be used in the entire downlink frame. After inserting some known pilots for the purpose of channel estimation at the MS, transmission occurs.

- *Downlink MS Optimization*—Upon reception on each MS, say $m$, the receiver will buffer signals in $M_t$ OFDM symbol durations, and use (20) to compute the receive weight vector. Finally, the estimates of the transmitted symbols are produced for detection [see (6)].

### V. SIMULATION RESULTS

Monte Carlo simulations have been carried out to assess the system performance of the proposed MIMO-OFDM broadcast system. Detailed simulation parameters are now summarized in Table 1. For convenience, we shall use the notation $\{n_T, [n_{R_1}, \ldots, n_{R_M}]\}$ to denote a broadcast MIMO system which has $n_T$ BS antennas and $M$ mobile users each with $n_{R_m}$ receive antennas.

Table 1: Simulation parameters

| | |
|---|---|
| Carrier frequency | 5 GHz |
| Sampling rate | 20 MHz |
| Number of subcarriers | $N = 64$ |
| FFT duration | 3.2 ns |
| Cyclic prefix duration | 0.8 ns |
| Symbol duration | 4 ns |
| Frame duration | 2 ms (500 OFDM symbols) |
| Modulation | QPSK |

In Figure 4, the average BER results for the PINV-MRC and PINV-MMSE are plotted against the average $E_b/N_0$ per branch-to-branch. The Doppler spread, $F_d$, is 80 Hz, which corresponds to a mobile moving at 17 km/h. The number of paths of the channel is 16 with an exponential power delay profile. We have set $M_t = 8$ and $M_f = 4$ for ML channel estimation. We provide results of $\{2, [2, 2]\}$, $\{3, [2, 2, 2]\}$ and $\{4, [2, 2, 2, 2]\}$ systems for both PINV-MMSE and PINV-MRC. Results show that PINV-MMSE performs significantly better than PINV-MRC. For PINV-MRC systems, there is always an irreducible error

floor because as the channel changes, the signals lose orthogonality and the CCI cannot be suppressed. Although the degradation is much reduced for PINV-MMSE, it also suffers from severe residual CCI causing irreducible error floor. The more the number of users in the system, the more the degradation.

Now if we set $F_d$ to be 40 Hz (speed of 8.5 km/h) and $L$ to be 4, then the channel becomes slowly varying. Results in Figure 5 demonstrate that good performance can be achieved with no irreducible error floor using PINV-MMSE (results of PINV-MRC are not provided here for conciseness). Results also indicate that the performances of the three configurations are more or less the same and that the system with more users will be a little better, which agrees with [12, 13] that multiuser diversity exists. In addition, results with perfect CSI are provided for comparison. As can be seen, although a shift of 6 dB occurs, the diversity (or the slope) preserves.

Figure 6 shows the results of MIMO-OFDM broadcast systems using PINV-MMSE for various number of MS antennas. Apparently, the performance of PINV-MMSE improves as the number of MS antennas increases even though it is more sensitive to the channel mismatch. In particular, at BER of $10^{-4}$, about 10 dB gain is possible as comparing $\{4, [2, 2, 2]\}$ system to $\{4, [1, 1, 1]\}$ system whereas there is about 7 dB difference between $\{4, [2, 2]\}$ system and $\{4, [1, 1]\}$ system.

As the system performance depends largely on the channel estimation. The pilot densities, $M_t$ and $M_f$, clearly affect the accuracy of channel estimation and hence the performance. To investigate the performance sensitivity to channel estimation error, we provide results of $\{4, [2, 2, 2, 2]\}$ for various values of $M_f$ with $M_t = 8$ in Figure 7. In this figure, the Doppler shift is further reduced to 8Hz in order to mitigate the effect of channel variance. As expected, with $M_f = 4$, the performance is improved as compared to the case when $M_f = 8$. Particularly, there is about 2.5 dB gain for every doubling the density of pilots. However, the more the pilots, the more the system overhead.

## VI. CONCLUSIONS

In this paper, we have proposed a robust OSDM scheme for MIMO-OFDM broadcast systems. By putting together the technologies of MIMO and OFDM, it has been shown to provide high-capacity (scalable to the number of BS antennas) high-data-rate wireless communications over time dispersive frequency selective fading channels. Simulation results have shown that though the system performance is sensitive to the Doppler spread, spectral reuse in spatial domain can still be accomplished to yield good performance.

## REFERENCES

[1] Y. Li, J. H. Winters, and N. R. Sollenberger, "MIMO-OFDM for wireless communications: signal detection with enhanced channel estimation," *IEEE Trans. Commun.*, vol. 50, no. 9, pp. 1471–1477, Sept. 2002.

[2] H. Bolcskei, M. Borgmann, and A. J. Paulraj, "Impact of the propagation environment on the performance of space-frequency coded MIMO-OFDM," *IEEE J. Select. Areas Commun.*, vol. 21, no. 3, pp. 427–439, Apr. 2003.

[3] H. Sampath, S. Talwar, J. Tellado, V. Erceg, and A. J. Paulraj, "A fourth-generation MIMO-OFDM broadband wireless system: design, performance, and field trial results," *IEEE Commun. Mag.*, vol. 40, no. 9, pp. 143–149, Sept. 2002.

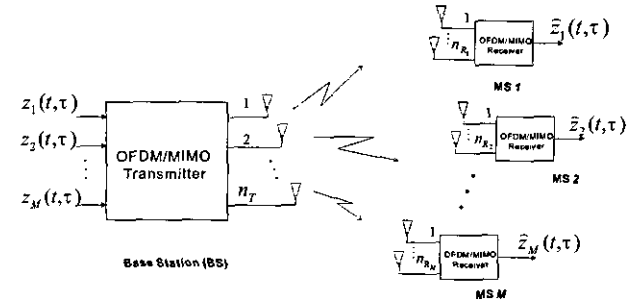[4] M. Costa, "Writing on dirty paper," *IEEE Trans. Info. Theory*, vol. 29, no. 3, pp. 439–441, May 1983.

[5] A. J. Goldsmith, and M. Effros, "The capacity region of broadcast channels with intersymbol interference and colored Gaussian noise," *IEEE Trans. Info. Theory*, vol. 47, no. 1, pp. 211–219, Jan. 2001.

[6] D. Tse and P. Viswanath, "On the capacity of the multiple antenna broadcast channel," in Proc. *DIMACS Series Discrete Math. and Theoretical Computer Science*, American Mathematical Society.

[7] G. J. Foschini, and A. H. Diaz, "Dirty paper coding: perturbing off the infinite dimensional lattice limit," in Proc. *DIMACS Series Discrete Math. and Theoretical Computer Science*, American Mathematical Society.

[8] W. Yu, and J. M. Cioffi, "Sum capacity of a Gaussian vector broadcast channel," submitted to *IEEE Trans. Info. Theory*.

[9] R. L. U. Choi, and R. D. Murch, "A transmit pre-processing technique for multiuser MIMO systems: a decomposition approach," to appear in *IEEE Trans. Wireless Commun.*.

[10] M. Rim, "Multiuser downlink beamforming with multiple transmit and receive antennas," *Elect. Letters*, vol. 38, pp. 1725–1726, Dec. 2002.

[11] Q. H. Spencer, and M. Haardt, "Capacity and downlink transmission algorithms for a multiuser MIMO channel," in Proc. *36th Asilomar Conf. Signals, Systems, and Computers*, Pacific Grove, CA, Nov. 2002.

[12] K. K. Wong, R. D. Murch, and K. Ben Letaief, "A joint-channel diagonalization for multiuser MIMO antenna systems," *IEEE Trans. Wireless Commun.*, vol. 4, no. 2, Jul. 2003.

[13] Z. G. Pan, K. K. Wong, and T. S. Ng, "MIMO antenna system for multiuser multi-stream orthogonal space division multiplexing,"in Proc. *Int. Conf. Commun.*, Anchorage, Alaska, U.S., 11-15 May 2003.

[14] J. Bingham, "Multicarrier modulation for data transmission: an idea whose time has come," *IEEE Commun. Mag.*, vol.28, pp.5-14, May 1990.

[15] G. H. Golub, and Charles F. Van Loan, *"Matrix computation,"* 2nd edition.

[16] D. X. Shen, Z. G. Pan, K. K. Wong, and V. O. K. Li, "Effective throughput: a unified benchmark for pilot-aided OFDM/SDMA wireless communication systems," in Proc. *IEEE Info. Commun.*, vol. 3, pp. 1603–1613, 30 Mar.-3 Apr. 2003.

Figure 1: System configuration of a MIMO-OFDM broadcast system.
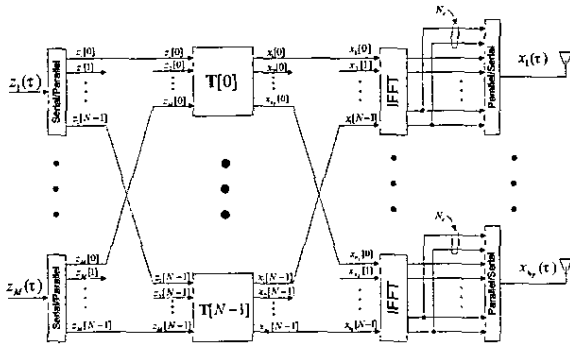
Figure 2: Transmitter structure of OFDM-MIMO at BS.
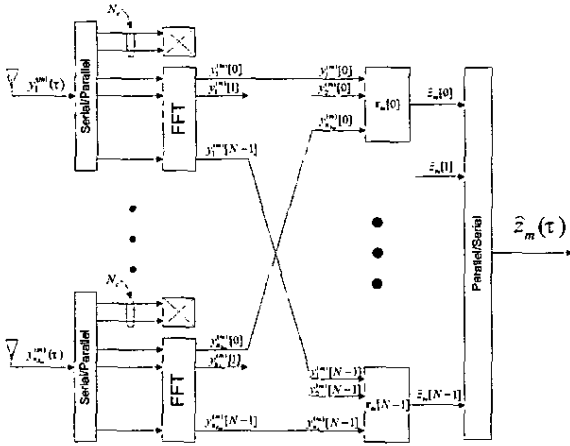


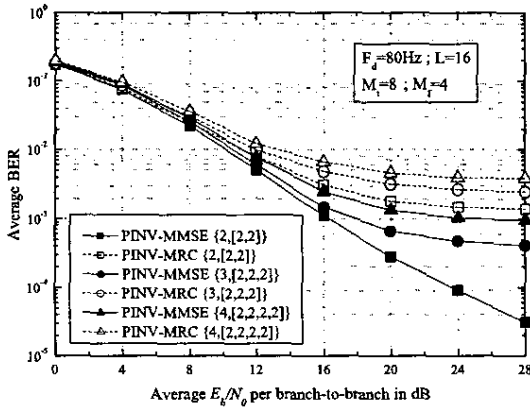Figure 3: Receiver structure of OFDM-MIMO at MS $m$.



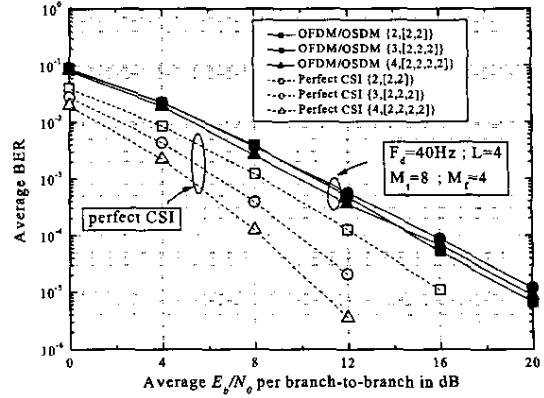Figure 4: Performance comparisons of PINV-MMSE and PINV-MRC in MIMO-OFDM systems.



Figure 5: Performance results of PINV-MMSE in MIMO-OFDM broadcast systems for various number of BS antennas.
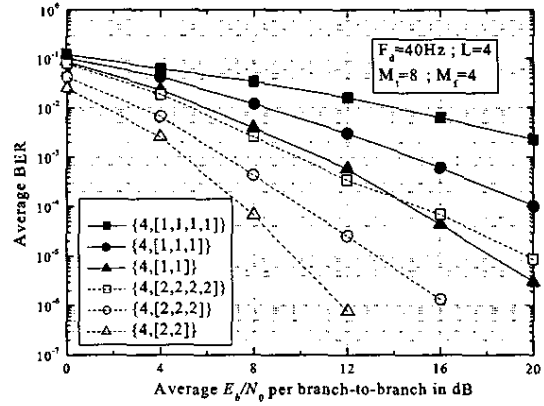


Figure 6: Performance results of PINV-MMSE in MIMO-OFDM broadcast systems for various number of MS antennas.
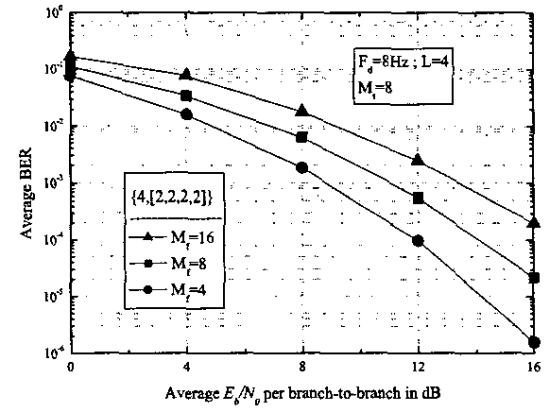


Figure 7: Performance results of PINV-MMSE in MIMO-OFDM broadcast systems with different pilot density in frequency domain.